

Article

Synergistic Effects of Curcumin and Nano-Curcumin against Toxicity, Carcinogenicity, and Oxidative Stress Induced by Tartrazine at Normal and Cancer Cell Levels

Gaber E. El-Desoky *, Saikh M. Wabaidur, Mohamed A. Habila  and Zeid A. AlOthman 

Department of Chemistry, College of Science, King Saud University, Riyadh 11451, Saudi Arabia; swabaidur@ksu.edu.sa (S.M.W.); mhabila@ksu.edu.sa (M.A.H.); zaothman@ksu.edu.sa (Z.A.A.)

* Correspondence: Geldesoky@ksu.edu.sa; Tel.: +96-65-9681-7646

Abstract: In this study, the cellular synergistic and antagonistic effects of mixing tartrazine (TZ) with curcumin (CUR) or curcumin-nanoparticles (CUR-NPs) were investigated. The in vivo administration of TZ, CUR, CUR-NPs, and TZ mixed with CUR or CUR-NPs at 75:25 or 50:50 ratios were tested. The results indicated that CUR and CUR-NPs reduced the cytotoxicity effects of TZ on skin fibroblast BJ-1 (ATCC[®] CRL-2522[™]) normal cells. However, among the tested materials, CUR-NPs had highest in vitro and in vivo antioxidant activity compared to TZ. Furthermore, CUR-NPs and CUR exhibited anticancer activity against HepG-2 liver cancer cells via apoptosis induction. The key apoptosis protein genes Caspase-3, p53, and Bax were upregulated, whereas Bcl-2, which exhibits anti-apoptosis activity, was downregulated. Our results indicated that the nano-formulation of CUR alters its physicochemical properties, including the size and shape, and increases its antioxidant and anticancer properties. CUR-NPs also overcome the side effect of using TZ as a yellow color and food preservative additive, due to its reduced toxicity, oxidative stress, and carcinogenicity. In agreement with our previous findings, CUR and CUR-NPs were able to protect against cellular oxidative stress by stimulating endogenous antioxidant defense enzymes, including superoxide dismutase (SOD), catalase (CAT), reduced glutathione (GSH), glutathione peroxidase (GPx), and glutathione-S-transferase (GST). We conclude that the nano-formulation of CUR exhibits economic benefits as a new strategy to use CUR as a food additive at the cellular level.

Keywords: food additives; tartrazine; curcumin; apoptosis; p53; oxidative stress; nano-curcumin



Citation: El-Desoky, G.E.; Wabaidur, S.M.; Habila, M.A.; AlOthman, Z.A. Synergistic Effects of Curcumin and Nano-Curcumin Against Toxicity, Carcinogenicity, and Oxidative Stress Induced by Tartrazine at Normal and Cancer Cell Levels. *Catalysts* **2021**, *11*, 1203. <https://doi.org/10.3390/catal11101203>

Received: 12 September 2021

Accepted: 28 September 2021

Published: 1 October 2021

Publisher's Note: MDPI stays neutral with regard to jurisdictional claims in published maps and institutional affiliations.



Copyright: © 2021 by the authors. Licensee MDPI, Basel, Switzerland. This article is an open access article distributed under the terms and conditions of the Creative Commons Attribution (CC BY) license (<https://creativecommons.org/licenses/by/4.0/>).

1. Introduction

In general, food additives are natural substances added in low concentrations to manufactured food in order to improve flavor, color, texture, and preservation [1]. A wide range of synthetic food additives have been used in food processing for economic purposes [2–4]. The FAO/WHO mark food additives with E code numbers for their worldwide identification [5,6]. Several reports indicated that some food additives exhibit human health side effects and place limits on their use [7,8]. In developing countries, there has been an increase in the use of synthetic colors due to their lower cost and stability [9]. Curcumin (CUR) is a widely available natural food colorant and preservative food additive extracted from turmeric (*Curcuma longa*). CUR displays several therapeutic properties, including antioxidant and anticancer activity [10,11]. Several in vivo and in vitro studies have reported that CUR exhibits a strong antioxidant effect against different forms of free radicals [12,13]. In addition, CUR exhibited high efficiency as an anti-inflammatory in vivo [10]. It has also been reported that CUR is a potent anticancer agent that reduces the proliferation of different human cancer cell lines via apoptosis induction, including that of HepG-2, Caco2, and MCF-7. Tartrazine (TZ; E102) is a synthetic yellow dye derived from coal tar that is used as a food additive and in pharmaceutical and cosmetic products. In developing countries, TZ is used as a saffron substitute [9–14]. The acceptable daily intake

(ADI) of TZ recommended by the Joint FAO/WHO Expert Committee on Food Additives (JECFA) is 0–7.5 mg/kg [15]. Several reports have indicated that TZ causes ROS generation and oxidative stress in vivo [16,17]. In this context, TZ also induces oxidative stress and causes cellular damage by inhibiting antioxidant defense enzymes and enhancing lipid peroxidation in vivo [18]. In this study, we examine the synergistic effects of curcumin and nano-curcumin as a natural food dye against the toxicity induced by TZ as a synthetic food dye at the cellular level.

2. Materials and Methods

2.1. Ethical Approval

This study was ethically approved by the Institutional Review Board of the Health Sciences Colleges Research on Human Subjects, King Saud University College of Medicine (E-20-4585) on 12 February 2020.

2.2. Chemicals and Supplies

All chemicals used in this study were purchased from Sigma (MA, USA) and Fluka (Buchs, Switzerland) and were of analytical grade.

2.3. Curcumin Nanoparticle Preparation

Curcumin loaded to nanoparticles were prepared according to the method described by [19] with slight modifications. In brief, 50 g polyethylene glycol 6000 (PEG 6000) were melted at 60 °C on a hotplate stirrer in a clean flask. While stirring, 10 g of curcumin dissolved into 15 mL of methylene chloride and 1 mL of Tween 80 was added dropwise to the melted PEG (10 drops/min). Then, the mixture was sonicated for 15 min using an ultrasonic processor. The mixture was allowed to cool at −4 °C for 24 h and completely ground in a refrigerated mortar. Finally, the product was sieved using a stainless-steel sieve (230 mesh), stored at 25 ± 0.5 °C in an airtight container, and used for the subsequent bioassay.

2.4. Nano-Curcumin Characterization

The morphology and particle size of the curcumin-NPs was visualized using a transmission electron microscope TEM (JEM 2100 HRT, Japan). The association level between curcumin and materials during nanoparticle production was evaluated using Fourier transform infrared spectroscopy FTIR (VERTEX 80v, Bruker, Germany) at 4 cm^{−1} resolution and a measurement scale range of 4000–400 cm^{−1} [20]. A particle size analyzer (Nano-ZS, Malvern Instruments Ltd., UK) was used to evaluate the surface charge of the NPs at 25 °C, as indicated by the zeta potential value; the NP dimensions, expressed in terms of Z-average size (d); and the polydispersity index (PDI).

2.5. Cytotoxicity and Anticancer

All the cell lines used in this study were obtained from the American Type Culture Collection (ATCC, Manassas, VA, USA). Colorectal adenocarcinoma (HCT-116, ATCC CCL-247) and hepatocellular carcinoma (HepG2, ATCC HB-8065) human cancer cell lines were used in this study, along with a normal cell line, skin fibroblast BJ-1 (ATCC CRL-2522). Cell lines were cultured in DMEM/high glucose supplemented with 2 mM L-glutamine, 10% FBS and 1% penicillin/streptomycin kept in a Corning 75 cm² u-shaped canted neck cell culture flask with vent cap (Corning, New York, NY, USA). Then, sub-confluent cultures (70–80%) were trypsinized (trypsin 0.05%/0.53 mM EDTA) and split depending on the seeding ratio [20,21].

2.6. MTT Assay for Cell Viability, Proliferation and Cytotoxicity

Cells (1 × 10⁵/well) were plated into 100 µL of medium/well in 96-well plates (Hi media). After 48 h incubation, the cell reached the confluence. Then, the media was replaced with RPMI-1640 media containing different concentrations (0.5, 1, 2.5, 5, and 10 µg/mL) of TZ, CUR, and CUR-NPs. After removal of the sample solution and washing with phosphate-

buffered saline (pH 7.4), 20 μL /well (5 mg/mL) of 0.5% 3-(4,5-dimethyl-2-thiazolyl)-2,5-diphenyltetrazolium bromide cells (MTT) phosphate-buffered saline solution was added. After 4 h incubation, 0.04 M HCl/isopropanol were added. Viable cells were determined by the absorbance at 570 nm with reference to absorbance at 655 nm. The concentration required for a 50% inhibition of viability (IC₅₀) was determined by graphical presentation. The absorbance at 570 nm was measured with a microplate reader (Bio-Rad, Richmond, CA, USA) using wells without samples containing cells as blanks. All experiments were performed in triplicate. The effect of the samples on the proliferation of cancer and normal cell lines was expressed as the cell viability using the following formula [22]:

$$\text{Cytotoxicity \%} = 100 - A_{570} \text{ of treated cells} / A_{570} \text{ of control cells} \times 100\%$$

2.7. Antioxidants Activity

2.7.1. 1-di-phenyl-picryl hydrazine (DPPH) Radical Scavenging Activity

The antioxidant activity of TZ, CUR, CUR-NPs and TZ mixed with CUR or CUR-NPs at 25:75 and 50:50 ratios was measured using the method of Shin (2012) with modifications. Briefly, 1 mL containing 5 μg of each sample or mixture was vortexed with 3 mL DPPH (0.004% dissolved in methanol). Then, the mixture was shaken and incubated under dark conditions at 37 °C for 30 min. The absorbance at 517 nm was measured, compared to vitamin C as a standard, and the scavenging activity was calculated using the following equation:

$$\text{DPPH}^\bullet \text{ scavenging activity (inhibition \%)} = [(A_c - A_s) / A_c] \times 100$$

where A_c is the absorbance of the DPPH solution and A_s is the absorbance of the sample.

2.7.2. In Vivo Antioxidant Activity

The total antioxidant potency was determined using a cellular antioxidant assay kit (Abcam ab242300) according to the manufacturer's instruction. In brief, HepG-2 and Bj-1 cells were seeded in a 96-well plate treated with 5 $\mu\text{g}/\text{mL}$ for each treatment compared to its respective control. After 24 h of treatment, cells were incubated with cell-permeable DCFH-DA fluorescence probe dye and the bioflavonoid Quercetin as a control. After incubation for 30 min, the cells were washed, and radical generation was initiated by adding Free Radical Initiator. The radical converted non-fluorescent DCFH-DA to highly fluorescent DCF. Higher antioxidant potency increases the scavenging for free radicals, and therefore inhibits DCF formation in a concentration-dependent manner. Thus, fluorescence is measured over time in a standard microplate fluorometer, and the antioxidant values were calculated by the following equation:

$$\text{In vivo antioxidant activity (\%)} = [(F_c - F_s) / F_c] \times 100$$

where F_c is the fluorescence of DCF and F_s is the fluorescence of the sample.

The antioxidant values were compared to Quercetin to determine the antioxidant activity within the cell.

2.7.3. Determination of p53, Bax, Caspase-3 and Bcl-2 Protein Levels

Cellular levels of the key apoptosis marker protein p53, caspase-3, Bax, and Bcl-2 were investigated 24 h post-treatment with the IC₅₀ of TZ, CUR, CUR-NPs and the TZ and CUR or CUR-NP mixture. Briefly, HepG-2 and Bj-1 cells were seeded at a concentration of 2×10^3 cells/well in 6-well plates for 24 h. The media were replaced by media containing treatments, and the incubation was continued for another 24 h. The collected cells were lysed and centrifuged at 10,000 rpm for 20 min at 4 °C. The protein concentration was measured in the supernatant by Bradford protein assay (8). A volume containing 50 μg of total protein was incubated with 5 mL of caspase substrate in 100 mL of the reaction buffer at 37 °C for 1 h in the dark. Caspase-3 activity was determined by a microplate

reader at 405 nm using a caspase-3 colorimetric assay kit (Abcam, ab39401) according to the manufacturer's instructions [23].

The *in vitro* protein level measurement of apoptotic marker p53, Bcl-2-associated X (Bax), and antiapoptotic marker B-cell lymphoma-2 (Bcl-2) in cell lysate was assessed by Enzyme-Linked Immunosorbent Assay Simple Step (ELISA) (ab207225, ab119506, and ab199080; Abcam) according to the manufacturer's instructions [24–26].

2.7.4. In Vivo Oxidative Stress Enzymes Determination

To test the effect of TZ, CUR, and CUR-NPs on the activity of oxidative stress enzymes *in vivo*, HepG-2 and BJ-1 cells were seeded in RPMI-1640 medium into cell culture flask plates (in quintuplicates), with 1×10^6 cells per flask, and incubated at 37 °C under a humidified atmosphere of 5% CO₂ for 48 h. The cell medium in the flasks was then changed to serum-free medium (SFM) containing 10 µL/mL of yogurt extract. After 48 h of incubation, the cell cultures were trypsinized (trypsin 0.05%/0.53 mM EDTA). The collected cells were washed in PBS, centrifuged at 2000 rpm for 5 min at 4 °C and resuspended in 1 mL PBS containing 0.1% Triton X-100. After sonication in a 1.5 mL microcentrifuge tube on ice for 2×10 s at 100 Hz (Vibra-cell, Sonics & Material), cells were centrifuged at 14,000 rpm for 30 min at 4 °C. Enzyme activity was tested in the supernatant. The cell culture enzyme activity of superoxide dismutase (SOD), catalase (CAT), reduced glutathione (GSH), and glutathione peroxidase (GPx) was determined according to the manufacturer's instructions of colorimetric kits ab65354, ab83464, ab142044, ab102530 Abcam, respectively.

2.8. Statistical Analysis

Data were statistically analyzed using the Costal statistical package data according to Anonymous (1989).

3. Results

3.1. CUR-NPs Characterization

3.1.1. Transmission Electron Microscope (TEM)

The results of TEM analysis indicated that the average particle size of CUR-NPs was 40 nm less than curcumin and the PEG-NPs control (Figure 1). Drug nano-formulations have been implicated in physicochemical alterations, e.g., of particle size, solubility, and shape. Such alterations elicit changes in various pharmaceutical characteristics, such as drug release patterns, efficiency, and cytotoxicity [19,27]. However, nanoparticles enhance drug delivery to target organisms and reduce the toxic effects on non-target organisms [28].

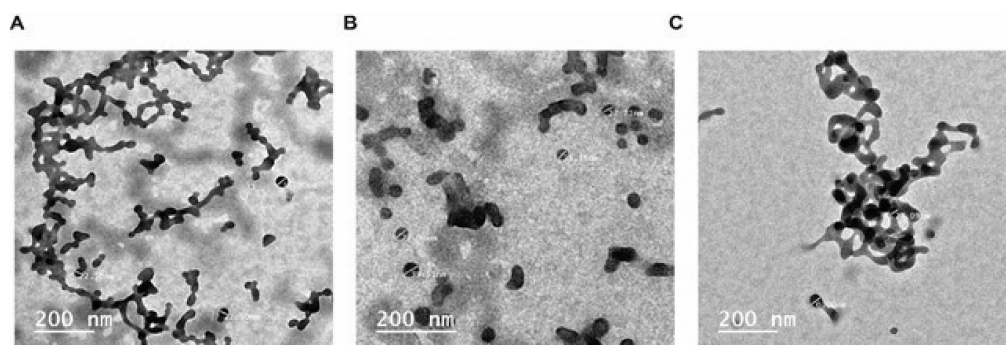


Figure 1. Transmission electron microscope TEM micrographs of unloaded control (left panel A), CUR-loaded PEG-NPs (right panel B and C).

3.1.2. Fourier-Transform Infrared Spectroscopy (FTIR)

The FTIR spectrum of PEG/CUR nanocomposites compared to curcumin are shown in Figure 2. The curcumin-loaded PEG shows the characteristic bands of the pure blend with some slight band shifts. These results indicate that the spectrum of PEG nano-carrier

bands was loaded in CUR-NPs. In addition, the spectrum of CUR showed two main peaks corresponding to the CUR spectrum loaded in CUR-NPs at 3512 and 1738 cm^{-1} . However, no new bands at the FTIR spectrum of CUR-NPs were observed compared to blank PEG-NPs, indicating that chemical reactions between CUR and other ingredients occurred. The stretching vibration at 3627 cm^{-1} corresponding to OH/NH₂ groups shifted to 3649 cm^{-1} , indicating that the CUR bonded to the functional groups of the PEG. As the peaks of the CUR-loaded nano-carrier spectrum overlapped with CUR and PEG-NPs, this shows that there was an interaction between CUR and the other nanomaterials.

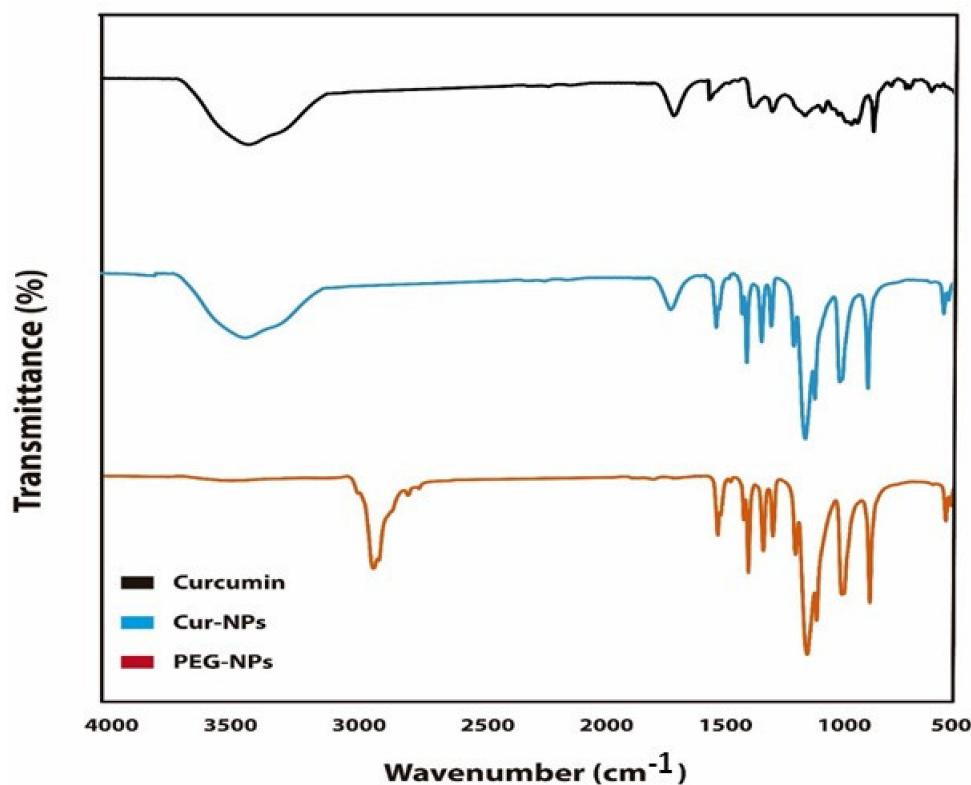


Figure 2. Fourier-transform infrared spectroscopy (FTIR) spectrum of CUR-NPs, CUR and PEG-NPs.

3.1.3. Particle Size Distribution

Particle size and zeta potential are a limiting factor of nano-medicine effectiveness in terms of drug delivery and stability levels. The zeta potential provides an indication of the surface charge of particles [29]. Analysis of the particle size (nm), PDI, and zeta potential (mV) revealed that the diameter of CUR-NPs and PEG-NPs was in the range of 360–393 nm. The discrete values of particle size, PDI, and zeta potential were 393.7 nm, 0.445, and -36.79 mV for CUR-NPs, and 360.9 nm, 0.588, and -33.50 mV for PEG-NPs, respectively.

3.1.4. Cytotoxic and Anticancer Activity

The cytotoxic and anti-proliferative potency of TZ, CUR, and CUR-NPs against HepG-2 cancerous cells and Bj-1 normal cells showed that TZ had a cytotoxic effect on Bj-1 normal cells, and a slightly cytotoxic effect was observed due to CUR treatment (Table 1). Thus, the nano-formulation of CUR reduced the cytotoxic effect of CUR. TZ exhibited anti-proliferation activity against HepG-2 cells, and CUR and CUR-NPs also inhibited cell growth. However, CUR-NPs showed a high cell mortality compared to curcumin. Taking into account the high cytotoxic activity of TZ, these results indicate that the nano-formulation improved the anticancer properties of CUR.

Table 1. Viability and cytotoxic activity of TZ, CUR and CUR-NPs.

*Concentration	0.5 µg/mL	1.0 µg/mL	2.5 µg/mL	5.0 µg/mL	10.0 µg/mL
Bj-1 Cells					
TZ	93.14 ± 2.15	89.94 ± 3.82	87.86 ± 3.44	77.29 ± 3.76	65.92 ± 2.15
CUR	96.01 ± 3.65	91.12 ± 2.14	87.98 ± 3.13	85.17 ± 3.85	79.13 ± 2.73
CUR-NPs	97.81 ± 3.11	95.71 ± 1.76	93.36 ± 2.22	91.05 ± 1.24	89.71 ± 2.42
HepG-2					
1-6 TZ	75.31 ± 1.35	72.23 ± 3.48	67.36 ± 4.93	48.97 ± 3.25	39.23 ± 2.96
CUR	68.1 ± 2.21	58.54 ± 2.31	46.36 ± 4.93	31.23 ± 2.01	16.06 ± 1.34
CUR-NPs	61.89 ± 3.02	50.13 ± 2.56	35.44 ± 2.15	22.23 ± 1.55	8.72 ± 1.06

*Media containing different concentrations (0.5, 1.0, 2.5, 5.0 and 10.0 µg/mL) of TZ, CUR and CUR-NPs.

3.1.5. Antioxidant Activity

In vitro antioxidant activity was measured by the potential scavenging of DPPH radicals. In this assay, we tested the scavenging activity of TZ mixed with CUR or CUR-NPs at ratios of 25:75 and 50:50 at 5 µg/mL compared to their respective controls. CUR-NPs displayed higher antioxidant activity compared to CUR and TZ (63.14% vs. 45.22% and 36.23%, respectively). CUR-NPs also increased the scavenging activity of TZ against DPPH radicals (Table 2). Increasing the mixing ratio to 50:50 in TZ:CUR-NPs ameliorated radical scavenging activity. The cellular antioxidant activity of Bj-1 and HepG-2 cells subjected to treatment was also tested, and the results indicated that in Bj-1 normal cells treated with CUR-NPs, cellular antioxidant activity was increased by about 30% compared to untreated cells. In BJ-1 cells, the highest cellular antioxidant activity occurred after 24 h of CUR-NPs treatment with antioxidant activity of 49.15%, followed by CUR treatment, which achieved an antioxidant activity of 26.49%, while TZ treatment exhibited the lowest antioxidant activity compared to the control. In agreement with previous in vitro antioxidant data, TZ mixed with CUR-NPs also showed an increase in the cellular antioxidant activity compared to TZ and TZ mixed with CUR, indicating that CUR-NPs and TZ act synergistically. By contrast, in HepG-2 cells, CUR has more cellular antioxidant activity either alone or mixed with TZ. However, nano-formulated CUR was mixed with the nanocarrier at a ratio of 1:5.

Table 2. In vitro and in vivo antioxidant capacity.

Sample	Bj-1 Cells	HepG-2	DPPH
Control	19.93 ± 2.43	23.43 ± 2.23	-
TZ	21.42 ± 2.02	20.35 ± 2.14	36.23 ± 2.90
CUR	26.49 ± 3.15	18.14 ± 2.06	45.22 ± 2.19
CUR-NPs	49.15 ± 3.12	13.78 ± 1.23	63.14 ± 3.04
TZ:CUR 75:25	31.32 ± 2.13	19.34 ± 1.40	43.24 ± 1.80
TZ:CUR-NPs 75:25	38.18 ± 3.75	17.15 ± 2.05	51.43 ± 3.12
TZ:CUR 50:50	37.41 ± 3.14	17.56 ± 1.11	49.26 ± 2.34
TZ:CUR-NPs 50:50	43.86 ± 3.25	14.78 ± 1.03	57.78 ± 1.03

TZ, CUR, Nano-CUR, TZ + CUR 75/25 (3.75 µg:1.25 µg), TZ + Nano-CUR 75/25 (3.75 µg:1.25 µg), TZ + CUR 50/50 (2.5 µg:2.5 µg), TZ + Nano-CUR 50/50 (2.5:2.5 µg).

3.1.6. Effects on Oxidative Stress Enzymes

In order to reduce cell stress, several cellular antioxidant markers are produced. We analyzed the impact of TZ, CUR, CUR-NPs, and their mixture on cellular antioxidant enzymes activity. The activity of superoxide dismutase (SOD), catalase (CAT), reduced glutathione (GSH), glutathione peroxidase (GPx), and glutathione-s-transferase GSH was determined in cell lysate of Bj-1 and HepG-2 after treatments with 5 µg/mL of substances alone or in a mixture. In Bj-1 normal cells, the levels of SOD, CAT, GSH, GPx, and GSH were slightly decreased ($p < 0.05$) after 48 h treatments with CUR and CUR-NPs compared to untreated cells (Table 3).

Table 3. Oxidative stress enzymes activity in Bj-1 and HepG-2 treated cells.

Bj-1					
Sample	SOD U/10 ⁶ Cells	Catalase U/10 ⁶ Cells	GSH U/10 ⁶ Cells	GPX U/10 ⁶ Cells	GST U/10 ⁶ Cells
Control	1.93 ± 0.21	87.58 ± 2.73	45.34 ± 2.00	34.14 ± 2.30	13.84 ± 1.15
TZ	1.12 ± 0.18	55.39 ± 2.84	29.23 ± 2.45	19.13 ± 2.15	7.21 ± 2.15
CUR	1.81 ± 0.16	81.24 ± 2.61	38.12 ± 2.49	27.92 ± 3.01	14.11 ± 1.09
CUR-NPs	1.89 ± 0.19	85.56 ± 2.34	58.14 ± 2.74	36.13 ± 2.81	12.23 ± 1.24
TZ:CUR 75:25	1.42 ± 0.33	59.67 ± 3.12	36.28 ± 2.67	24.27 ± 2.27	7.98 ± 1.27
TZ:CUR-NPs 75:25	2.18 ± 0.25	64.35 ± 2.55	43.25 ± 3.02	29.25 ± 3.13	8.15 ± 1.12
TZ:CUR 50:50	1.67 ± 0.29	66.76 ± 3.10	41.21 ± 2.54	31.21 ± 3.23	9.89 ± 1.44
TZ:CUR-NPs 50:50	1.86 ± 0.19	79.98 ± 3.13	47.18 ± 2.73	35.28 ± 3.11	11.38 ± 1.31
HepG-2					
Control	2.75 ± 0.35	55.32 ± 3.12	22.25 ± 1.39	25.36 ± 1.78	17.02 ± 1.33
TZ	2.32 ± 0.45	49.46 ± 2.17	19.17 ± 2.43	17.45 ± 2.01	9.76 ± 0.86
CUR	2.88 ± 0.49	67.34 ± 2.25	43.49 ± 3.12	31.67 ± 1.78	24.82 ± 1.58
CUR-NPs	3.12 ± 0.63	73.32 ± 3.64	48.06 ± 2.55	39.37 ± 1.62	28.09 ± 2.11
TZ:CUR 75:25	3.21 ± 0.72	61.39 ± 3.31	39.37 ± 1.96	26.32 ± 1.84	21.94 ± 2.31
TZ:CUR-NPs 75:25	3.97 ± 0.65	67.78 ± 2.78	56.64 ± 2.87	30.18 ± 2.05	25.05 ± 1.24
TZ:CUR 50:50	2.67 ± 0.41	72.32 ± 2.32	49.76 ± 2.62	37.38 ± 2.62	26.17 ± 1.65
TZ:CUR-NPs 50:50	2.66 ± 0.39	82.43 ± 4.01	57.24 ± 3.05	43.23 ± 2.08	29.86 ± 2.05

A significant reduction in the activity levels of all enzymes was observed with the TZ treatment alone, but when TZ was mixed with CUR or CUR-NPs, the enzyme activity levels were significantly increased (Table 3). In the case of HepG-2, an increase in the oxidative stress markers was observed, with the exception of cells treated with TZ. These findings suggest that CUR and CUR-NPs have a synergistic effect with TZ and reduce the levels of oxidative stress protection markers. These results were in agreement with the anticancer and antioxidant data that were obtained.

3.1.7. Apoptotic Marker Protein Levels in Bj-1 and HepG-2 Treated Cells

It was hypothesized that anticancer activity is associated with apoptosis induction. Apoptosis is a process controlled by several signal transduction pathways including p53, Bax, caspase-3, and Bcl-2 proteins. In this context, the protein levels of p53, Bax, and Caspase-3 protein markers were determined in Bj-1 and HepG-2 cells exposed to 5 µg/mL of TZ, CUR, CUR-NPs, TZ:CUR 75:25, TZ:CUR-NPs 75:25, TZ:CUR 50:50, and TZ:CUR-NPs 50:50 compared with untreated cells (Table 4).

Table 4. Apoptosis marker protein levels in HepG-2 and Bj-1 treated cells.

Bj-1				
Sample	Caspas-3 pg.mL ⁻¹	P53 pg.mL ⁻¹	Bax pg.mL ⁻¹	Bcl-2 ng.mL ⁻¹
Control	59.11 ± 1.82	76.13 ± 2.34	21.12 ± 1.11	2.12 ± 0.34
TZ	73.87 ± 2.33	93.23 ± 3.21	48.18 ± 3.24	3.13 ± 0.52
CUR	57.01 ± 3.31	81.32 ± 2.15	27.11 ± 2.43	2.34 ± 0.16
CUR-NPs	58.83 ± 2.27	74.23 ± 2.76	28.34 ± 1.88	2.23 ± 0.24
TZ:CUR 75:25	68.32 ± 2.87	88.32 ± 4.32	24.12 ± 1.65	2.51 ± 0.54
TZ:CUR-NPs 75:25	66.54 ± 3.21	79.35 ± 2.36	26.04 ± 2.13	3.05 ± 0.53
TZ:CUR 50:50	63.34 ± 1.96	82.32 ± 2.19	21.289 ± 1.33	2.41 ± 0.45
TZ:CUR-NPs 50:50	60.02 ± 1.48	77.98 ± 3.04	24.15 ± 1.09	2.56 ± 0.12
HepG-2				
Control	68.23 ± 4.23	85.24 ± 3.17	31.34 ± 3.43	2.44 ± 0.57
TZ	85.02 ± 3.15	88.13 ± 3.45	39.69 ± 2.98	2.17 ± 0.35
CUR	113.81 ± 4.13	136.12 ± 4.35	61.64 ± 3.11	1.72 ± 0.55
CUR-NPs	141.19 ± 3.78	168.04 ± 5.34	86.26 ± 3.64	1.09 ± 0.04
TZ:CUR 75:25	89.62 ± 4.33	113.28 ± 3.17	57.37 ± 3.82	1.78 ± 0.12
TZ:CUR-NPs 75:25	104.38 ± 4.25	132.45 ± 3.97	66.35 ± 3.24	1.45 ± 0.17
TZ:CUR 50:50	103.67 ± 3.78	129.97 ± 5.14	69.24 ± 3.45	1.47 ± 0.24
TZ:CUR-NPs 50:50	126.96 ± 4.24	147.12 ± 3.96	81.68 ± 3.53	0.79 ± 0.06

By contrast, exposure to the abovementioned compounds or mixtures significantly reduced Bcl-2. Our data also indicated that CUR and CUR-NPs are able to ameliorate the side effects of TZ, thereby decreasing TZ cytotoxicity and enhancing apoptosis induction.

4. Discussion

Turmeric has long been recognized for its pharmaceutical properties and utility as a food colorant. In addition, turmeric is a major source of CUR. It is a polyphenolic compound that has been shown to exhibit antioxidant and anti-inflammatory properties to treat metabolic syndromes, arthritis, anxiety, and hyperlipidemia. It has long been used as a natural yellow color additive in foods. However, several synthetic yellow color agents have also been used in food processing as an alternative to CUR. Many reports have highlighted the side effects of these synthetic compounds, among which is tartrazine, the most commonly used synthetic yellow color as a replacement for CUR. In this study, we compared CUR and TZ in terms of their pharmaceutical benefits and cytotoxicity, and nano-formulated CUR was also investigated.

We used TEM, FTIR, and zeta sizer to characterize CUR-NPs. TEM analysis indicated that the size of CUR-NPs ranged from 35 to 100 nm and its surface morphology was smooth and homogenous (Figure 1). The TEM results also indicated that curcumin nanoparticles are homogeneously distributed in the polymer matrix [30]. FTIR spectrum analysis indicated that curcumin was loaded into PEG and the spectrum has showed an integration between PEG and CUR. However, the FTIR spectrum of the CUR-NPs did show some differences from pure PEG-NPs (Figure 2). By comparing the spectrum of curcumin with CUR-NPs, two absorption peaks at 3512 and 1738 cm^{-1} , corresponding to $-\text{OH}$ and $-\text{NH}$ stretching vibrations, shifted to 3620 and 1821 cm^{-1} in the CUR-NPs spectrum. Previous reports indicated that the FTIR spectrum of curcumin shows a peak at 3417 cm^{-1} that could be attributed to the phenolic $-\text{OH}$ stretching bands. Two sharp peaks at 2920 and 2852.2 cm^{-1} were ascribed to CH Stretching. The bands at 1706 cm^{-1} and 1641 cm^{-1} were due to C=O and C=C stretching, respectively. In addition, the bands at 1464, 1105, and 723 cm^{-1} were ascribed to $-\text{OH}$ vibrations, C-O-C stretching modes, and cis $-\text{CH}$ vibrations of the aromatic ring [31]. All these results reflect the chemical interaction between CUR and PEG.

In this study, the cell viability of BJ-1 and HepG-2 indicated that CUR-NPs have the strongest anticancer activity against HepG-2 Cells, followed by CUR and TZ. Moreover, TZ exhibited the strongest cytotoxic effect against BJ-1 normal cells (Table 1). The observed anticancer activity against HepG-2 was specific, as marginal growth inhibition was observed for BJ-1 normal cells. Similar results have been reported in a previous study that tested the effect of CUR on the same HepG-2 hepatocarcinoma cell line that we studied [31].

We analyzed the antioxidant, anticancer, and oxidative stress enzyme induction of CUR-NPs in comparison with CUR and TZ in vitro and in vivo. Curcumin has been shown to improve the cytotoxic, antioxidant, and anticancer effects of synthetic food additive TZ [32]. The levels of oxidative stresses protection enzymes in the cell lysate of BJ-1 and HepG-2 treated with CUR-NPs, CUR, and TZ are shown in Table 3. The nano-formulated CUR showed high potential for increased protection against oxidative enzymes compared to the control. It has been reported that CUR increases antioxidant enzymes in the blood such as superoxide dismutase (SOD) [32,33]. Many reports have found a significant effect of purified curcuminoid supplementation on oxidative stress parameters including plasma activities of SOD and catalase, and serum concentrations of glutathione peroxidase (GSH) and lipid peroxides [33]. Notably, all of the studies included in that meta-analysis utilized some sort of formulation to overcome bioavailability challenges, and four out of the six used piperine. Several mechanisms are responsible for curcumin's effect on free radicals. It can scavenge different forms of free radicals, such as reactive oxygen species (ROS) and reactive nitrogen species (RON); modulate the activity of GSH, catalase, and SOD enzymes active in the neutralization of free radicals; and inhibit ROS-generating enzymes, such as lipoxygenase/cyclooxygenase and xanthine hydrogenase/oxidase [34,35]. In addition,

CUR is a lipophilic compound, which makes it an efficient scavenger of peroxy radicals. Therefore, like vitamin E, CUR is also considered a chain-breaking antioxidant [36].

In this study, protein levels of pro and anti-apoptotic results revealed that the CUR-NPs and CUR mediated cytotoxic effect against HepG-2 cells proceeds by apoptosis induction, as shown by the significant upregulation of pro-apoptotic marker proteins p53, Caspase-3, and Bax (Table 4). Apoptosis is genetically controlled by either an intrinsic or extrinsic pathway, both of which culminate in the proteolytic activation of caspase-3, the last enzyme that executes the characteristic hallmarks of apoptosis such as DNA fragmentation; phosphatidylserine exposure, which causes reversion of the plasma membrane; and the degradation of nuclear protein [37]. The effects of plant-derived phytochemicals have long been suggested to be mediated by the induction of apoptosis and cell cycle arrest [22,38].

5. Conclusions

In this study, cellular synergistic and antagonistic effects of mixing CUR and CUR-NPs with TZ were investigated against different cell lines. The combination of nano-CUR with TZ overcame the side effects associated with using TZ alone. The cytotoxic activity of TZ was improved by the application of the nano-formulation of CUR. The synergistic effect of CUR and CUR-NPs with TZ reduced the levels of oxidative stress protection markers. The obtained data also indicated that CUR and CUR-NPs were able to ameliorate the side effects of TZ by decreasing its cytotoxicity and enhancing apoptosis induction. CUR and CUR-NPs were able to protect against cellular oxidative stress by stimulating endogenous antioxidant defense enzymes. We conclude that the nano-formulation of curcumin has potential as a new strategy for using CUR as a food additive at the cellular level.

Author Contributions: Formal analysis, S.M.W.; investigation, G.E.E.-D.; project administration, Z.A.A.; data curation, M.A.H. All authors have read and agreed to the published version of the manuscript.

Funding: This research was funded by [King Abdul-Aziz City for Science and Technology (KACST)] grant number [2-17-01-001-0080].

Data Availability Statement: Not applicable.

Acknowledgments: The authors are grateful to King Abdul-Aziz City for Science and Technology (KACST) for Financially Supporting Project No. (2-17-01-001-0080), Riyadh, Saudi Arabia.

Conflicts of Interest: The authors declare no conflict of interest.

References

1. Tawfek, N.; Amin, H.; Abdalla, A.; Fargali, S. Adverse effects of some food additives in adult male albino rats. *Curr. Sci. Int.* **2015**, *4*, 525–537.
2. AlFaris, N.A.; ALTamimi, J.Z.; ALOthman, Z.A.; Al Qahtani, S.F.; Wabaidur, S.M.; Ghfar, A.A.; Aldayel, T.S. Analysis of aflatoxins in foods retailed in Saudi Arabia using immunoaffinity column cleanup and high-performance liquid chromatography-fluorescence detection. *J. King Saud Uni. Sci.* **2020**, *32*, 1437–1443. [\[CrossRef\]](#)
3. AlFaris, N.A.; Wabaidur, S.M.; Alothman, Z.A.; Altamimi, J.Z.; Aldayel, T.S. Fast and efficient immunoaffinity column cleanup and liquid chromatography–tandem mass spectrometry method for the quantitative analysis of aflatoxins in baby food and feeds. *J. Sep. Sci.* **2020**, *43*, 2079–2087. [\[CrossRef\]](#)
4. Bhowmick, S.; AlFaris, N.A.; ALTamimi, J.Z.; ALOthman, Z.A.; Aldayel, T.S.; Wabaidur, S.M.; Islam, M.A. Screening and analysis of bioactive food compounds for modulating the CDK2 protein for cell cycle arrest: Multi-cheminformatics approaches for anticancer therapeutics. *J. Mol. Struct.* **2020**, *1216*, 128316. [\[CrossRef\]](#)
5. Carocho, M.; Barreiro, M.; Morales, P.; Ferreira, I. Adding molecules to food, Pros and Cons: A review on synthetic and natural food additives. *Compr. Rev. Food Saf. Food Saf.* **2014**, *13*, 377–399. [\[CrossRef\]](#)
6. Abdel Ghany, T. Safe food additives: Review. *J. Biol. Chem. Res.* **2015**, *32*, 402–437.
7. Amin, K.; Al-Shehri, F. Toxicological and safety assessment of tartrazine as a synthetic food additive on health biomarkers: A review. *Afr. J. Biotechnol.* **2018**, *17*, 139–149.
8. Pressman, P.; Clemens, R.; Hayes, W.; Chanda, R. Food additive safety: A review of toxicologic and regulatory issues. *Toxicol. Res. Appl.* **2017**, *1*, 1–22. [\[CrossRef\]](#)

9. Ali, A.; Abdelgayed, S.H.; El-Tawil, O.; Bakeer, A. Toxicological and histopathological studies on the effect of tartrazine in male albino rats. *Int. J. Biol. Biomol. Agric. Food Biotechnol. Eng.* **2016**, *10*, 513–518.
10. Alsamydai, A.; Jaber, N. Pharmacological aspects of Curcumin: Review article. *Int. J. Pharmacogn.* **2018**, *5*, 313–326.
11. El-Desoky, G.E.; Wabaidur, S.M.; AlOthman, Z.A.; Habila, M.A. Regulatory Role of Nano-Curcumin against Tartrazine-Induced Oxidative Stress, Apoptosis-Related Genes Expression, and Genotoxicity in Rats. *Molecules* **2020**, *25*, 5801. [[CrossRef](#)] [[PubMed](#)]
12. Hewlings, S.; Kalman, D. Curcumin: A review of its effects on human health. *Foods* **2017**, *6*, 92. [[CrossRef](#)]
13. Jovicic, D.; Jozinovic, A.; Grcevic, M.; Aleksovska, E.; Subaric, D. Nutritional and health benefits of Curcumin. *Nutr. Health Benefits* **2017**, *6*, 22–27.
14. Khayyat, L.; Essawy, A.; Sorour, J.; Soffar, A. Tartrazine induces structural and functional aberrations and genotoxic effects in vivo. *Peer J.* **2017**, *5*, 1–14. [[CrossRef](#)] [[PubMed](#)]
15. Himri, I.; Bellahcen, S.; Souana, F.; Belmekki, F.; Aziz, M.; Bnouham, M.; Zoheir, J.; Berkia, Z.; Mekhfi, H.; Saalaoui, E. A 90-Day oral toxicity study of tartrazine, a synthetic food dye, in Wistar rats. *Int. J. Pharm. Pharm. Sci.* **2011**, *3*, 159–169.
16. Boussada, M.; Lamine, J.; Bini, I.; Abidi, N.; Lasrem, M.; El-Fazaa, S.; El-Golli, N. Assessment of a sub-chronic consumption of tartrazine (E102) on sperm and oxidative stress features in Wistar rat. *IFRJ* **2017**, *24*, 1473–1481.
17. El-Desoky, G.E.; Abdel-Ghaffar, A.; Al-Othman, Z.A.; Habila, M.A.; Al-Sheikh, Y.A.; Ghneim, H.K.; Giesy, J.P.; Aboul-Soud, M.A. Curcumin protects against tartrazine-mediated oxidative stress and hepatotoxicity in male rats. *Eur. Rev. Med. Pharmacol. Sci.* **2017**, *21*, 635–645.
18. Morales, A.; Pérez-Jiménez, A.; Hidalgo, C.; Abellan, E.; Cardenete, G. Oxidative stress and antioxidant defenses after prolonged starvation in Dentex dentex liver. *Comp. Biochem. Physiol. C Toxicol. Pharmacol.* **2004**, *139*, 153–161. [[CrossRef](#)]
19. González, J.O.W.; Gutiérrez, M.M.; Ferrero, A.A.; Band, B.F. Essential oils Nano formulations for stored-product pest control—Characterization and biological properties. *Chemosphere* **2014**, *100*, 130–138. [[CrossRef](#)] [[PubMed](#)]
20. Aboul-Soud, M.A.M.; Ashour, A.E.; Challis, J.K.; Ahmed, A.F.; Kumar, A.; Nassrallah, A.; Alahmari, T.A.; Saquib, Q.; Siddiqui, M.A.; Al-Sheikh, Y.; et al. Biochemical and Molecular Investigation of in Vitro Antioxidant and Anticancer Activity Spectrum of Crude Extracts of Willow Leaves *Salix safsaf*. *Plants* **2020**, *9*, 1295. [[CrossRef](#)]
21. El-Hallouty, S.M.; Soliman, A.A.; Nassrallah, A.; Salamatullah, A.; Alkaltham, M.S.; Kamal, K.Y.; Hanafy, E.A.; Gaballa, H.S.; Aboul-Soud, M.A.M. Crude Methanol Extract of Rosin Gum Exhibits Specific Cytotoxicity against Human Breast Cancer Cells via Apoptosis Induction. *Anti-Cancer Agents Med. Chem.* **2020**, *20*, 1028–1036. [[CrossRef](#)] [[PubMed](#)]
22. Abo-Salem, H.M.; Nassrallah, A.; Soliman, A.A.F.; Ebied, M.S.; Elawady, M.E.; Abdelhamid, S.A.; El-Sawy, E.R.; Al-Sheikh, Y.A.; Aboul-Soud, M.A.M. Synthesis and Bioactivity Assessment of Novel Spiro Pyrazole-Oxindole Congeners 358 Exhibiting Potent and Selective in vitro Anticancer Effects. *Molecules* **2020**, *25*, 1124. [[CrossRef](#)]
23. Mosmann, T. Rapid colorimetric assay for cellular growth and survival: Application to proliferation and cytotoxicity assays. *J. Immunol. Methods* **1983**, *65*, 55–63. [[CrossRef](#)]
24. Bradford, M.M. A rapid and sensitive method for the quantitation of microgram quantities of protein utilizing the principle of protein-dye binding. *Anal. Biochem.* **1976**, *72*, 248–254. [[CrossRef](#)]
25. Hirao, A.; Kong, Y.Y.; Matsuoka, S.; Wakeham, A.; Ruland, J.; Yoshida, H.; Liu, D.; Elledge, S.J.; Mak, T.W. DNA damage-induced activation of p53 by the checkpoint kinase Chk2. *Science* **2000**, *287*, 1824–1827. [[CrossRef](#)]
26. Ottoni, O.; Cruz, R.; Alves, R. Efficient and simple methods for the introduction of the sulfonyl, acyl and alkyl protecting groups on the nitrogen of indole and its derivatives. *Tetrahedron* **1998**, *54*, 13915–13928. [[CrossRef](#)]
27. Chen, C.J.; Makino, S. Murine coronavirus replication induces cell cycle arrest in G0/G1 phase. *J. Virol.* **2004**, *78*, 5658–5669. [[CrossRef](#)]
28. De Oliveira, J.L.; Campos, E.V.R.; Bakshi, M.; Abhilash, P.C.; Fraceto, L.F. Application of nanotechnology for the encapsulation of botanical insecticides for sustainable agriculture: Prospects and promises. *Biotechnol. Adv.* **2014**, *32*, 1550–1561. [[CrossRef](#)] [[PubMed](#)]
29. Gogos, A.; Knauer, K.; Bucheli, T.D. Nanomaterials in plant protection and fertilization: Current state, foreseen applications, and research priorities. *J. Agric. Food Chem.* **2012**, *60*, 9781–9792. [[CrossRef](#)] [[PubMed](#)]
30. Kamel, N.A.; Mansour, S.H.; Abd-El-Messieh, S.L.; Khalil, W.A.; Abd-El Nour, K.N. Biophysical properties of PPF/HA nanocomposites reinforced with natural bone powder. *Adv Mat. Res.* **2015**, *4*, 145–164. [[CrossRef](#)]
31. Dash, M.; Chiellini, F.; Ottenbrite, R.M.; Chiellini, E. Chitosan—A versatile semi-synthetic polymer in biomedical applications. *Prog. Polym. Sci.* **2011**, *36*, 981–1014. [[CrossRef](#)]
32. Kamel, N.A.; Abd-El-Messieh, S.L.; Neveen, M.S. Chitosan/banana peel powder nanocomposites for wound dressing application: Preparation and characterization. *Mat. Sci. Eng.* **2017**, *72*, 543–550. [[CrossRef](#)]
33. Zhao, Z.; Xie, M.; Li, Y.; Chen, A.; Li, G.; Zhang, J.; Hu, H.; Wang, X.; Li, S. Formation of Curcumin nanoparticles via solution-enhanced dispersion by supercritical CO₂. *Int. J. Nanomed.* **2015**, *10*, 3171. [[CrossRef](#)]
34. Duvoix, A.; Blasius, R.; Delhalle, S.; Schneckeburger, M.; Morceau, F.; Henry, E.; Dicato, M.; Diederich, M. Chemopreventive and therapeutic effects of Curcumin. *Cancer Lett.* **2005**, *223*, 181–190. [[CrossRef](#)] [[PubMed](#)]
35. Gunes, H.; Gulen, D.; Mutlu, R.; Gumus, A.; Tas, T.; Topkaya, A.E. Antibacterial effects of Curcumin: An in vitro minimum inhibitory concentration study. *Toxicol. Ind. Health* **2016**, *32*, 246–250. [[CrossRef](#)] [[PubMed](#)]

36. El-Houssiny, A.S.; Ward, A.A.M.; Mansour, S.H.; Abd-El-Messieh, S.L. Biodegradable blends based on polyvinyl pyrrolidone for insulation purposes. *J. App. Poly. Sci.* **2012**, *124*, 3879–3891. [[CrossRef](#)]
37. El-Nashar, D.E.; Rozik, N.N.; Soliman, M.; Helaly, F. Study the release kinetics of Curcumin released from PVA/Curcumin composites and its evaluation towards hepatocarcinoma. *J. App. Pharm. Sci.* **2016**, *6*, 67–72. [[CrossRef](#)]
38. Motawie, A.M.; Mansour, N.A.; Kandile, N.G.; Abd-El-Messieh, S.L.; El-Mesallamy, S.M.; Sadek, E.M. Study on the Properties of Carbon Reinforced Unsaturated Thermoset Polyester Resin Nanocomposites. *Aust. J. Basic Appl. Sci.* **2016**, *1*, 37–47. [[CrossRef](#)]